J Low Temp Phys (2008) 151: 927–933
DOI 10.1007/s10909-008-9769-7

A TDMA Hybrid SQUID Multiplexer

C.D. Reintsema · J. Beall · W. Doriese · W. Duncan · L. Ferreira · G.C. Hilton · K.D. Irwin · D. Schmidt · J. Ullom · L. Vale · Y. Xu

Received: 23 July 2007 / Accepted: 5 October 2007 / Published online: 25 January 2008

Abstract We have developed a multiplexed read-out for transition-edge sensors (TES) based on a hybrid time- and frequency-domain basis set, similar to that used in time-division multiple-access (TDMA) mobile phones. The hybrid basis set uses bandwidth more efficiently than microwave frequency-division SQUID multiplexing, making it possible to multiplex more detectors in each output line. The high open-loop bandwidth provided by our SQUID TDMA system also makes it possible to multiplex large arrays of fast, high dynamic range detectors such as fast x-ray calorimeters. In this approach, we embed the second-stage SQUID amplifier of our standard time-division multiplexer in an impedance matching circuit coupled to a broadband cryogenic high electron mobility transistor (HEMT) in a microwave reflectometer configuration. The input signals are flux coupled into the first-stage SQUID amplifiers whose signals are time-division multiplexed into the second-stage SQUID. At room temperature, the signal from the HEMT is mixed down to dc for analysis and further signal processing.

Keywords SQUID · Multiplexer · Cryogenic array readout

PACS 85.25.Dq · 85.25.-j

1 Introduction

SQUID time-division multiplexing (SMUX) is a well developed method for reading out multiple transition-edge sensors in a single amplifier channel. In time-division multiplexing, SQUIDs coupled to detectors are turned on at separate times and read out in a common amplifier channel. NIST has been developing and refining SQUID time-division multiplexers over the last decade [1–3].

C.D. Reintsema (✉) · J. Beall · W. Doriese · W. Duncan · L. Ferreira · G.C. Hilton · K.D. Irwin · D. Schmidt · J. Ullom · L. Vale · Y. Xu
National Institute of Standards & Technology, 325 Broadway, Boulder, CO 80305, USA
e-mail: reintsema@boulder.nist.gov

In frequency-division multiplexing schemes, all pixels in an array are operated simultaneously, each at a unique excitation frequency. Frequency-division SQUID multiplexing schemes have been developed at a few megahertz by the use of a single SQUID coupled to an array of TESs modulated at different frequencies [4].

NIST has demonstrated frequency-division SQUID multiplexing at microwave frequencies using both dc and dissipationless ac SQUIDs [5, 6]. Microwave SQUID multiplexers can have frequency selectivity sufficient to fit many thousands of SQUIDs in an octave bandwidth from 4–8 GHz in a single HEMT amplifier. However, fabrication deviations in the resonance frequency of ±2 MHz (2σ) [7] limit the practical number of SQUIDs per HEMT to 1,000–2,000 if line overlaps are not tolerated. A further stage of multiplexing within a single microwave resonator has the potential to greatly increase the number of low-frequency detectors that can be multiplexed.

Hybrid SQUID multiplexing schemes have been proposed that use the available bandwidth more efficiently than do basic time- or frequency-division methods. Proposed basis sets include hybrids of frequency- and time-division multiplexing [8] and the implementation of two stages of frequency-division multiplexing [9]. TDMA multiplexing uses a hybrid basis set that combines the beneficial attributes of TDM and FDM in a hybrid scheme to more efficiently utilize the available bandwidth. TDMA is utilized extensively in cell phone technology. Here we demonstrate TDMA SQUID multiplexing using a conventional time-division SQUID multiplexer chip in a microwave resonant circuit.

2 Experiment

In this experiment we excited the second-stage SQUID with a microwave tone at 0.1–1.0 GHz and measured the amplitude of the reflected signal with a high-bandwidth low-noise cryogenic HEMT. As shown in Fig. 1, we accomplished this by using a simple L-section matching network between the second-stage SQUID on the SMUX chip and the HEMT input. A discrete 10 pF capacitor (C_R in Fig. 1) was embedded across the leads to the second-stage SQUID, and the wire bonds to the chip provided an estimated 4 nH of inductance (L_R in Fig. 1), thereby establishing the impedance matching criteria. The L-section resonator was designed to match a second-stage SQUID dynamic resistance of approximately 3 Ω to the 50 Ω input impedance of a HEMT at an operating frequency of 0.5 GHz (mid-band for the HEMT).

The experimental platform for these measurements was a custom dip probe immersed in liquid helium (4 K). On the printed circuit board (PCB) in close proximity to the SMUX chip was the discrete capacitor that, in combination with the wire bonds to the second-stage SQUID on the SMUX chip, implemented the impedance matching circuit. From the matching circuit a controlled-impedance microstrip led to the SMA feed-through to the HEMT. On the microwave side of the probe a reflectometer was configured from a directional coupler and the cryogenic HEMT amplifier. The HEMT amplifier had a useable band from 0.1 to 1.0 GHz and a noise temperature of 12–15 K across this band. A room temperature microwave amplifier provided further gain and fed the reflected signal into the rf port of a mixer. A homodyne scheme was

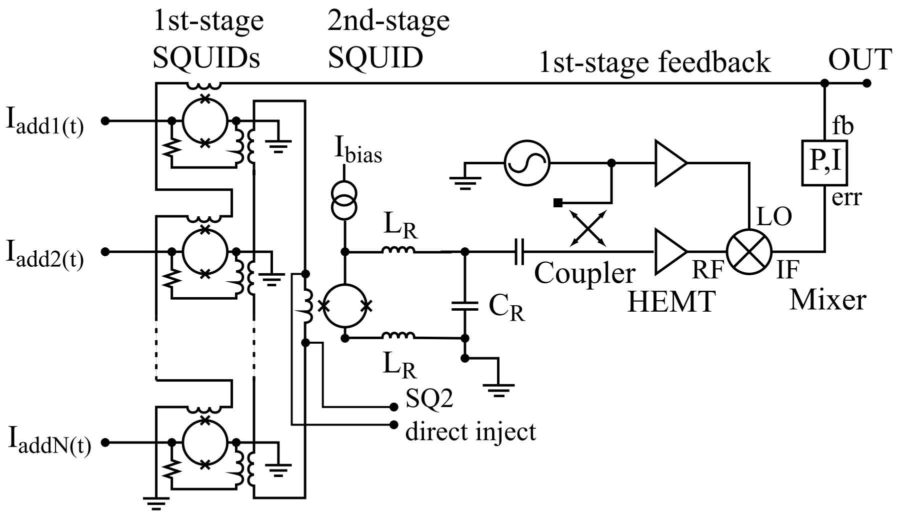

Fig. 1 A circuit schematic showing the SMUX on the *left*, the discrete L_R and C_R of the matching circuit, the cryogenic HEMT and rf signal chain, and the digital feedback system for closed-loop TDMA operation

employed to extract the amplitude of the reflected voltage wave at one phase. This extracted signal was then directly sampled for time-domain measurements, or provided to the digital feedback card input for closed-loop TDMA operation.

Also located on the PCB were SMA connectors for the second-stage SQUID feedback, the common first-stage SQUID feedback, and the row address lines for the first two rows of the SMUX circuit. These high-speed lines allowed us for the first time to characterize the intrinsic on-chip frequency response and bandwidth of the SMUX circuit. The pole that limits the bandwidth (sampling rate) in typical time-division applications is an off-chip pole resulting from parasitic inductance in cryogenic wiring leads between the second-stage SQUID (on the detector cold stage at ~ 80 mK adjacent to the TES detectors) and the SQUID series array input coil (on the 4 K stage). The ratio of this inductance to the second-stage SQUID dynamic resistance gives an L/R roll-off below 2 MHz. The intrinsic on-chip bandwidth of the SQUID TDM circuitry is significantly higher, as we demonstrated in this experiment.

Basic verification of the overall system functionality is indicated in the response curves of Fig. 2. This family of curves shows reflected microwave signal amplitude versus magnetic flux (modulated current into the second-stage SQUID input coil) for varying second-stage SQUID bias. Response to flux modulation in the second-stage SQUID was observed at frequencies from 0.1 to 0.8 GHz. The highlighted curve indicates the bias conditions used for successive measurements.

3 Results and Discussion

A demonstration of TDMA multiplexing is shown in Fig. 3a. We used the NIST digital feedback electronics [10] to operate four first-stage SQUIDs in a flux locked

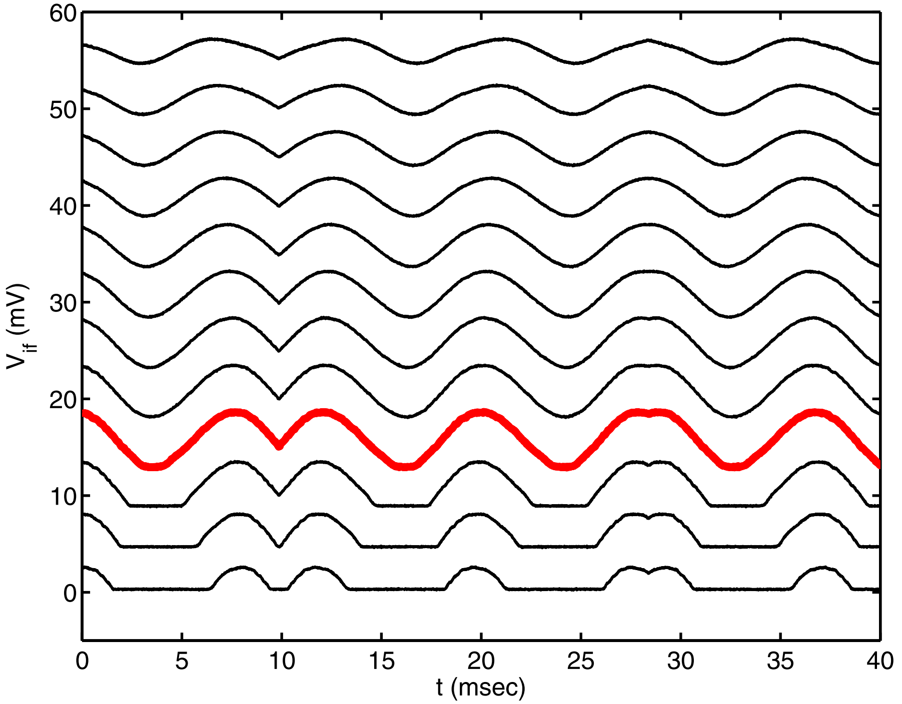

Fig. 2 (Color online) A family of demodulated voltage versus flux curves for the second-stage SQUID. The curves are offset upwards for increasing second-stage SQUID bias. The 0.541 GHz excitation signal was applied at a power level of −61.6 dBm

loop. The row address currents were switched at a frequency of 781.25 kHz for this demonstration. On two of the channels, sine and triangle wave signals from function generators were used to directly couple flux into the first-stage SQUID input coils specific to these channels. The signal shown in Fig. 3a is the multiplexed feedback signal from the NIST electronics. The sine and triangle wave components of this signal are clearly visible. The other two channels had no stimulus applied, therefore their signals are the dc feedback voltage necessary to maintain the lock point.

A secondary goal of this experiment was to measure the intrinsic frequency response of the 1 × 32 SMUX. This information is essential to determine the current capability of the SMUX and to aide in realizing practical modifications to the circuit to broaden the bandwidth. This is especially relevant to pure TDM where the maximum switching speed limits the applicability of this technology as array formats grow. The switching speed is also important in TDMA where we desire to know how many detector channels can fit in a single resonator channel and, ultimately, the scale of array that can be read-out using this approach.

At demodulated frequencies up to 20 MHz, amplitude measurements of the modulated intermediate frequency (IF) signal were made. This was done by direct sampling of the IF waveform in the time domain using a high-speed data-acquisition

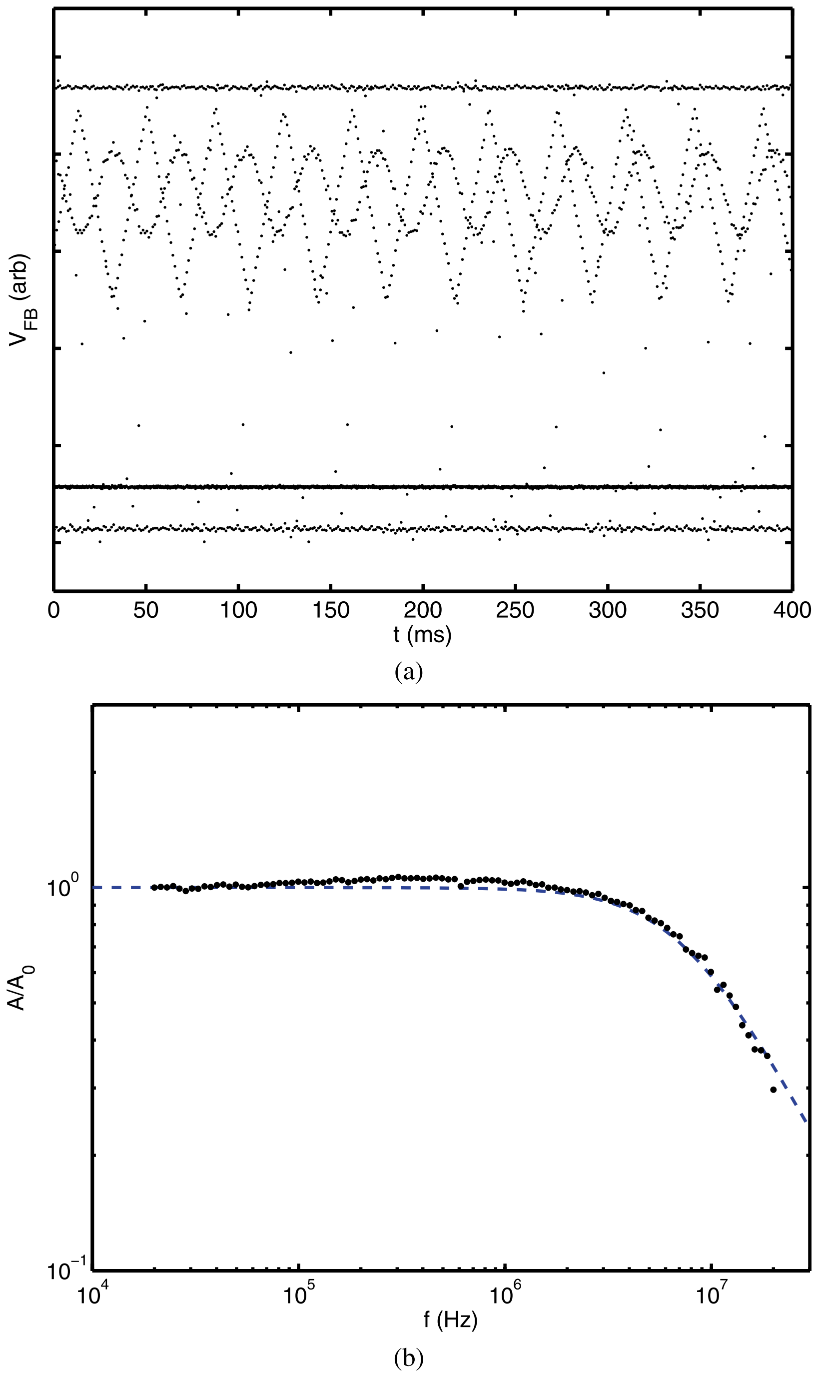

Fig. 3 (**a**) Digital feedback signal amplitude versus time for closed loop TDMA operation. (**b**) Reflected microwave signal amplitude ratio versus flux modulation frequency for the second stage SQUID

system. The waveform amplitude was measured as a function of increasing second-stage SQUID feedback frequency. A plot of amplitude ratio versus flux modulation frequency is shown in Fig. 3b. A 1-pole frequency response fit to this data (dashed line on plot) yields a 3 dB point of 7.1 MHz. This pole is consistent with calculated values for the bandwidth of direct flux injection into the second-stage SQUID input coil. This is an explicit measure of the on-chip bandwidth of the common coupling coil between the first-stage SQUIDs and the input to the second-stage SQUID. If desired, this bandwidth can be widened in future designs by reducing the coupling between the SQUID stages at the cost of a degradation in white noise level referred to the first-stage SQUID input.

The noise floor of the TDMA multiplexer was determined using a calibrated reference tone at 1 kHz. The noise floor, $\sim 2\mu\phi_0/\sqrt{\mathrm{Hz}}$ as referred to the second-stage SQUID input, was consistent with the noise level that we typically expect from this generation of SQUID chips at 4 K, and is dominated by the Johnson noise of the intra-coil damping resistors in the SQUIDs.

4 Summary

We have demonstrated TDMA multiplexed operation in a closed-loop configuration. Operation in this mode provides high slew rates, and may be ideal for fast X-ray calorimeter measurements. However, it requires a feedback line to be provided to every column of time-division multiplexed SQUIDs. In the future, we will implement flux-ramp modulation of the SQUIDs [7] to eliminate the need for separate feedback wires. Common address wires will still be required. Thus, if 32 time-division multiplexed SQUIDs are attached to each microwave resonator, 32 low-frequency address lines will be required, independent of the total number of microwave resonators. This approach should make it possible to multiplex more than 10,000 low-frequency detectors per HEMT amplifier.

Acknowledgement The authors acknowledge Konrad Lehnert of JILA for his help and assistance in both this experiment and those that preceded it.

References

1. J.A. Chervenak, K.D. Irwin, E.N. Grossman, J.M. Martinis, C.D. Reintsema, Appl. Phys. Lett. **74**, 4043–4045 (1999)
2. P.A.J. de Korte, J. Beyer, S. Deiker, G.C. Hilton, K.D. Irwin, M. MacIntosh, N. Sae Woo, C.D. Reintsema, L.R. Vale, M.E. Huber, Rev. Sci. Instrum. **74**, 3807–3815 (2003)
3. W.B. Doriese, J.N. Ullom, J.A. Beall, W.D. Duncan, L. Ferreira, G.C. Hilton, R.D. Horansky, K.D. Irwin, J.A.B. Mates, C.D. Reintsema, L.R. Vale, Y. Xu, B.L. Zink, M.W. Rabin, A.S. Hoover, C.R. Rudy, D.T. Vo, Appl. Phys. Lett. **90** (2007)
4. J. Yoon, J. Clark, J. Gildemeister, A. Lee, M. Myers, P. Richards, J. Skidmore, Appl. Phys. Lett. **78**, 371–373 (2001)
5. K.D. Irwin, K.W. Lehnert, Appl. Phys. Lett. **85**, 2107–2109 (2004)
6. J.A.B. Mates, G.C. Hilton, K.D. Irwin, L.R. Vale, K.W. Lehnert, Appl. Phys. Lett. (2007, submitted)
7. K.W. Lehnert, K.D. Irwin, M.A. Castellanos-Beltran, J.A.B. Mates, L.R. Vale, IEEE Trans. Appl. Supercond. **17**, 705–709 (2007)

8. K.D. Irwin, J.A. Beall, W.B. Doriese, W.D. Duncan, G.C. Hilton, J.A.B. Mates, C. Reintsema, D.R. Schmidt, J.N. Ullom, L.R. Vale, B.L. Zink, K.W. Lehnert, Nucl. Instrum. Methods Phys. Res. A **559**, 802–804 (2006)
9. I. Hahn, P.K. Day, B. Bumble, H.G. LeDuc, J. Mod. Phys. D (2007, submitted)
10. C.D. Reintsema, J. Beyer, N. Sae Woo, S. Deiker, G.C. Hilton, K. Irwin, J. Martinis, J. Ullom, L.R. Vale, M. MacIntosh, Rev. Sci. Instrum. **74**, 4500–4508 (2003)